International Journal Of Innovative Trends In Multi Disciplinary Scientific Research
ISSN (Online): 3139 – 2687
(www.ijtmsr.co.in) Volume 9, Issue 6, 2026

Design and Comparative Structural Analysis of Conveyor Belt Materials under Tension and Pressure Loads

Vemavarapu Sai Kumar[1], T.Vasantha[2]

[1]PG scholar, Department of Mechanical engineering, Gonna Institute of Information Technology & Sciences, Visakhapatnam, India.
[2]Assistant professor, Department of Mechanical engineering, Gonna Institute of Information Technology & Sciences, Visakhapatnam, India.

Abstract

Belt conveyor systems are extensively employed in mining, thermal power plants, and bulk material handling industries for the efficient transportation of materials over long distances. The structural performance of conveyor belts is essential for ensuring reliable operation, reducing maintenance requirements, and extending service life. In this study, a coal transportation conveyor belt system was designed and analyzed to investigate the effect of different belt materials on its structural performance. A three-dimensional model of the conveyor assembly, including the belt, rollers, idlers, and supporting frame, was developed in CATIA using actual design specifications and imported into ANSYS Workbench for finite element analysis. Four widely used belt materials—Balata, Nylon 66, PVC, and Reinforced Rubber—were evaluated under identical tension and pressure loading conditions. The analysis focused on total deformation and equivalent (von Mises) stress in both the belt and idler components. The simulation results revealed noticeable variations in deformation among the selected materials, while the stress values under tension loading remained nearly the same. Among all the materials investigated, PVC demonstrated the best structural performance by exhibiting the minimum deformation (20.12 mm under tension and 11.5 mm under pressure with idler support) along with the lowest idler stress of 38 MPa. These findings indicate that PVC is a suitable belt material for improving the stiffness, durability, and overall structural performance of coal-handling conveyor systems.

Keywords: Belt conveyor, finite element analysis, PVC, Nylon 66, Balata, reinforced rubber, tension load, pressure load, equivalent stress, total deformation.

I. INTRODUCTION

A belt conveyor is one of the most widely used and efficient bulk-material handling systems employed in industries such as mining, thermal power generation, cement manufacturing, ports, and steel plants. It consists of two or more pulleys with a continuous belt looped around them; one pulley, the drive pulley, is powered, while the other, the idler pulley, rotates freely. Compared with conventional material handling methods, belt conveyors provide higher reliability, greater carrying capacity, continuous material flow, and lower energy consumption, and can be arranged in horizontal, inclined, or combined configurations depending on plant layout.

In the coal handling plant of a typical integrated steel plant, belt conveyors are responsible for transporting coal from unloading stations and storage yards to processing units. Because coal is a primary raw material for the steel-making process, uninterrupted and reliable conveyor operation is essential. During service, the conveyor belt and its supporting rollers experience continuous tensile and pressure loading arising from belt tension and the weight of the conveyed material. Excessive deformation or stress in the belt can cause misalignment, spillage, increased wear, and unplanned downtime; therefore, the selection of an appropriate belt material and rigorous structural evaluation are essential design considerations.

International Journal Of Innovative Trends In Multi Disciplinary Scientific Research
ISSN (Online): 3139 – 2687
(www.ijtmsr.co.in) Volume 9, Issue 6, 2026

This paper presents a finite element based comparative structural analysis of four commonly used conveyor belt materials — Balata, Nylon 66, Polyvinyl Chloride (PVC), and Reinforced Rubber — under tension and pressure loading conditions representative of an actual coal-handling conveyor. A three-dimensional model of the conveyor assembly was developed in CATIA and analyzed in ANSYS Workbench to determine the total deformation and equivalent stress developed in the belt and idler components, with the objective of identifying the material offering the best combination of stiffness, strength, and dimensional stability for industrial coal-handling applications.

II. RELATED WORK

Conveyor system selection and component optimization have been studied extensively. Fonseca et al. [1] proposed an expert system for conveyor equipment selection, while Nuttall et al. [2] developed a viscoelastic model of rolling friction in wheel-driven belt conveyors. Lan [3] introduced an optimization model for multi-conveyor manufacturing systems, and Shinde and Patil [4] applied finite element analysis to optimize conveyor rollers, shafts, and support structures for weight reduction. Opasiak et al. [5] presented an improved roller design to reduce rolling resistance and power consumption.

Several studies have focused on idler and roller resistance and the associated energy consumption: Lu and Li [6] developed a regression model for idler rotational resistance; Kulinowski et al. [8], [9] investigated the influence of bearing design and testing methods on energy consumption; and Król and Kisielewski [15], [23] and Kulinowski and Kasza [24] examined field-measured idler loads and energy efficiency in mining conveyors. Kou et al. [7] proposed a belt-conveyor-based parallel storage system, and Gładysiewicz et al. [10] combined experimental and FEM–DEM modelling to study dynamic belt deflection. Kieckhafer et al. [11] developed a life-cycle-cost design approach for multiple-drive conveyors.

Dynamic behavior, vibration, and control of conveyor systems have also received considerable attention, including startup optimization under non-uniform loading [12], permanent-magnet suspension conveyors [13], multi-body dynamic modelling [14], non-uniform bulk-material distribution and speed control [16], and lumped-parameter and viscoelastic dynamic models of belt drives [17]–[22]. More recently, Li et al. [25] investigated sensor-based monitoring and predictive maintenance for improving conveyor reliability. While these studies address conveyor selection, dynamics, and energy efficiency in depth, comparatively fewer works directly compare the structural (deformation and stress) response of alternative belt materials under identical loading using finite element analysis — the gap addressed in the present work.

III. CONVEYOR SYSTEM AND DESIGN PARAMETERS

The belt conveyor assembly considered in this study consists of a conveyor belt, drive and tail pulleys, troughing and return idlers, and a supporting steel frame. The conveyor belt is the primary load-carrying medium and is subjected to tensile stress from belt tension and pressure loading from the conveyed coal. The drive pulley transmits power from the motor–gearbox unit to the belt through friction, while the tail pulley redirects the belt from the carrying side to the return side. Troughing idlers, spaced at regular intervals, support the belt on the carrying side and shape it into a trough to increase capacity and reduce spillage, whereas return idlers support the empty belt on the return run. The frame, fabricated from structural steel sections, transfers all operating loads to the foundation and must resist bending, shear, and deflection under service conditions.

TABLE I. DESIGN PARAMETERS OF THE CONVEYOR SYSTEM

Parameter	Symbol	Value
Material	—	Coal
Bulk density	ρ	1.7 T/m³
Lump size	—	0–10 mm
Belt width	B	1850 mm

International Journal Of Innovative Trends In Multi Disciplinary Scientific Research
ISSN (Online): 3139 – 2687
(www.ijtmsr.co.in) Volume 9, Issue 6, 2026

Conveyor capacity	C	800–900 TPH
Conveyor length	L	29 m
Lift height	H	5.112 m
Belt speed	V	1.2 m/s
Troughing angle	λ	35°
Conveyor inclination	θ	10.36°
Top-side load	W_1	33,400 N
Bottom-side load	W_2	60,690 N

Based on these specifications, the belt cross-sectional area required for a design capacity of 900 TPH was calculated from $Q = 3600 \cdot A \cdot V \cdot \rho$, giving $A = 0.1225$ m² and a corresponding mass flow rate of 250 kg/s. The total load acting on the conveyor, obtained as the sum of the top- and bottom-side loads ($W = W_1 + W_2$), was 94,090 N, equivalent to a distributed load of 3244.5 N/m over the 29 m conveyor length. Resolving this load along the 10.36° incline gave a vertical component of 16.90 kN and a horizontal component of 92.56 kN, corresponding to a power requirement of 20.28 kW (a 30 kW motor was recommended for the drive). The support reactions were calculated as 47.05 kN at each end, and the maximum bending moment on the conveyor structure, obtained from $M_{max} = wL^2/8$, was 341.06 kN·m. These parameters formed the basis for the geometric model and the loading conditions applied in the finite element analysis described in Section IV.

IV. FINITE ELEMENT METHODOLOGY

A. Geometric Modelling

A three-dimensional model of the conveyor belt assembly, comprising the belt, support rollers, and idlers, was developed in CATIA based on the design parameters listed in Table I. The geometry was subsequently imported into ANSYS Workbench, where minor simplifications were made to reduce computational cost without affecting the accuracy of the structural results.

B. Material Properties

Four belt materials — Balata, Nylon 66, PVC, and Reinforced Rubber — were considered for comparison, while structural steel was assigned to the rollers and idlers. Young's modulus, Poisson's ratio, and density for each material are listed in Table II. Among the belt materials, PVC possesses the highest Young's modulus (3.37 GPa), indicating the greatest inherent stiffness, while Reinforced Rubber has the lowest (1.47 GPa).

TABLE II. MATERIAL PROPERTIES USED IN THE FE MODEL

Material	E (GPa)	Poisson's ratio	Density (kg/m³)
Balata	1.84	0.30	1100
Nylon 66	1.99	0.39	1180
PVC	3.37	0.35	1450
Reinforced Rubber	1.47	0.40	1400
Steel (rollers/idlers)	210	0.30	7850

C. Meshing

The conveyor assembly was discretized using three-dimensional tetrahedral elements, which are well suited to the curved surfaces of the belt, rollers, and idlers. An element size of approximately 10 mm was used, resulting in a mesh of 20,276 elements and 5,261 nodes (Fig. 1), providing an appropriate balance between accuracy and computational cost. Mesh quality was verified in terms of element aspect ratio and skewness, with additional refinement near roller contacts and load-application regions.

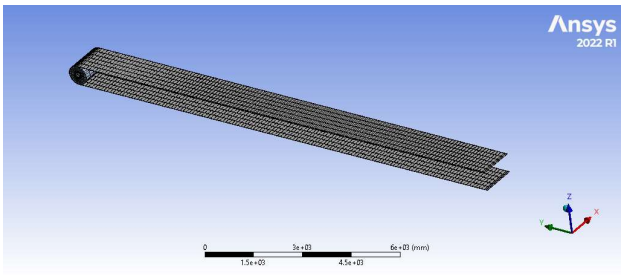


Fig. 1. Finite element mesh of the conveyor belt assembly (20,276 elements, 5,261 nodes).

International Journal Of Innovative Trends In Multi Disciplinary Scientific Research
ISSN (Online): 3139 – 2687
(www.ijtmsr.co.in) Volume 9, Issue 6, 2026

D. Boundary Conditions and Loading

Fixed supports were applied at the roller mounting locations to represent the actual support conditions, and bonded contact was defined between the belt and roller surfaces to ensure proper load transfer. A rotary displacement boundary condition was applied at the drive roller to simulate the driving action of the motor–gearbox unit (Fig. 2). Operational loads of 33,400 N and 60,690 N, corresponding to the top (carrying) and bottom (return) sides of the belt respectively, were applied to represent the combined effect of belt tension and the conveyed coal, giving a total applied load of 94,090 N consistent with Section III. Separate simulations were carried out for each belt material under identical boundary and loading conditions, first under tension loading directly on the belt, and subsequently under pressure loading with two idler supports included in the model, to evaluate the influence of idler support on belt deformation and stress.

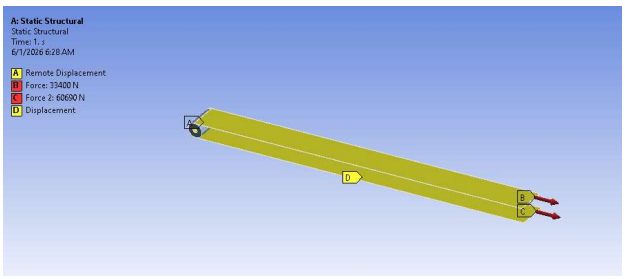


Fig. 2. Boundary conditions and load application on the conveyor belt.

V. RESULTS AND DISCUSSION

A. Deformation and Stress under Tension Loading

Under the applied tension load, the maximum deformation in every material occurred at the unsupported (free) end of the belt, while the minimum deformation occurred near the roller support locations, reflecting the imposed boundary constraints. Table III summarizes the maximum total deformation obtained for each material.

TABLE III. BELT DEFORMATION UNDER TENSION LOAD

Material	Deformation (mm)
Balata	38.43
Nylon 66	33.00
PVC	20.12
Reinforced Rubber	44.40

PVC exhibited the lowest deformation (20.12 mm), while Nylon 66, Balata, and Reinforced Rubber showed 33.00 mm, 38.43 mm, and 44.40 mm respectively — increases of 39.1%, 91.0%, and 120.7% relative to PVC. Fig. 3 shows the deformation contour obtained for PVC, confirming the expected gradient from the fixed roller region toward the free end.

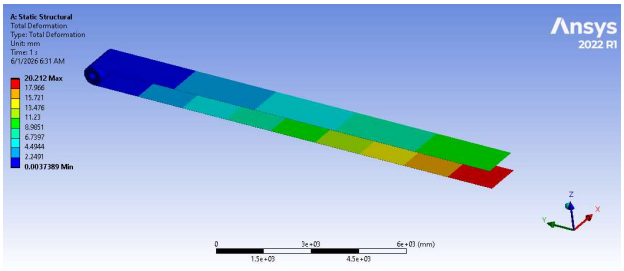


Fig. 3. Total deformation of the PVC belt under tension loading (max. 20.21 mm).

The corresponding equivalent (von Mises) stress results are summarized in Table IV. Unlike deformation, stress showed very little variation between materials, with Balata recording the highest value (5.50 MPa) against 5.40 MPa for the remaining three materials — a difference of only 1.85%. This indicates that under tension loading, stress in the belt is governed primarily by the applied load and geometry rather than material stiffness, whereas deformation is strongly influenced by material stiffness. Fig. 4 shows the corresponding stress contour for PVC, with the peak value (5.49 MPa) occurring at the belt–roller contact region.

International Journal Of Innovative Trends In Multi Disciplinary Scientific Research
ISSN (Online): 3139 – 2687
(www.ijtmsr.co.in) Volume 9, Issue 6, 2026

TABLE IV. BELT STRESS UNDER TENSION LOAD

Material	Stress (MPa)
Balata	5.50
Nylon 66	5.40
PVC	5.40
Reinforced Rubber	5.40

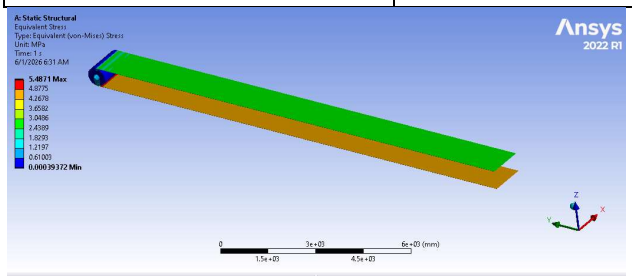


Fig. 4. Equivalent (von Mises) stress in the PVC belt under tension loading (max. 5.49 MPa).

B. Deformation and Stress under Pressure Loading (with Idler Supports)

A second set of simulations incorporated two idler supports beneath the belt and applied a pressure load on the top surface to represent the conveyed coal. As expected, the addition of idler supports substantially reduced overall belt deformation relative to the tension-load case, with the maximum deformation occurring in the unsupported belt span between idlers. Table V lists the resulting deformation values.

TABLE V. BELT DEFORMATION UNDER PRESSURE LOAD (WITH IDLERS)

Material	Deformation (mm)
Balata	20.00
Nylon 66	19.34
PVC	11.50
Reinforced Rubber	26.00

PVC again produced the lowest deformation (11.50 mm), compared with 19.34 mm for Nylon 66 (+68.2%), 20.00 mm for Balata (+73.9%), and 26.00 mm for Reinforced Rubber (+126.1%). Fig. 5 shows the deformation contour for the PVC belt over the idler geometry, clearly illustrating the trough profile between the two idler supports.

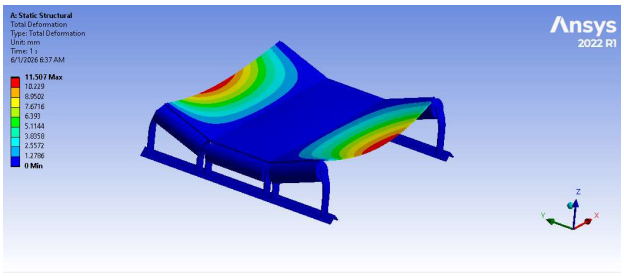


Fig. 5. Total deformation of the PVC belt with idler supports under pressure loading (max. 11.51 mm).

The equivalent stress developed in the idlers under pressure loading, summarized in Table VI, showed a clearer dependence on belt material than the tension-load case, because the stiffer belt materials distribute load to the idlers differently. PVC produced the lowest idler stress (38 MPa), while Nylon 66, Balata, and Reinforced Rubber produced 49 MPa (+28.9%), 52 MPa (+36.8%), and 56 MPa (+47.4%) respectively.

TABLE VI. IDLER STRESS UNDER PRESSURE LOAD

Material	Stress (MPa)
Balata	52
Nylon 66	49
PVC	38
Reinforced Rubber	56

C. Comparative Discussion

Combining the deformation and stress results from both loading cases, PVC consistently produced the lowest deformation and the lowest (or equal-lowest) stress among the four materials studied, indicating superior stiffness and dimensional stability. Since belt stress under tension loading was found to be governed mainly by the applied load rather than material properties, deformation and idler stress under pressure loading are the more discriminating criteria for material selection. On this basis, PVC offers the best combination of dimensional stability, reduced idler loading, and structural reliability for the coal-handling

conveyor considered in this study, while Reinforced Rubber — despite its widespread use for flexibility and impact resistance — showed the highest deformation and stress in all cases.

VI. CONCLUSION

A conveyor belt system used for coal transportation was modelled in CATIA and analyzed in ANSYS Workbench to compare the structural performance of four belt materials — Balata, Nylon 66, PVC, and Reinforced Rubber — under tension and pressure loading. Under tension loading, PVC showed the lowest deformation (20.12 mm) against 33.00 mm, 38.43 mm, and 44.40 mm for Nylon 66, Balata, and Reinforced Rubber respectively, while belt stress varied only marginally across materials (5.40–5.50 MPa). Under pressure loading with idler supports, PVC again produced the lowest deformation (11.50 mm) and the lowest idler stress (38 MPa), compared with up to 26.00 mm deformation and 56 MPa idler stress for Reinforced Rubber. These results confirm that PVC possesses superior stiffness and dimensional stability, making it the most suitable material among those studied for conveyor belt applications in industrial coal-handling systems. Future work may include experimental validation through fabrication and physical testing, evaluation of additional materials such as aramid-fibre-reinforced and hybrid polymer composites, dynamic and fatigue-life analysis under cyclic loading, and structural optimization of belt thickness, idler spacing, and support geometry to further improve conveyor performance and service life.

REFERENCES

[1] D. J. Fonseca, G. Uppal, and T. J. Greene, "Development of an expert system for conveyor selection," Int. J. Prod. Res., vol. 42, pp. 1–15, 2004.

[2] A. J. G. Nuttall, G. Lodewijks, and A. J. Klein Breteler, "Modeling rolling friction in wheel-driven belt conveyors," Bulk Solids Handling, vol. 26, pp. 48–56, 2006.

[3] C. H. Lan, "Optimization of multi-conveyor systems in manufacturing," Int. J. Prod. Econ., vol. 84, pp. 255–267, 2003.

[4] S. M. Shinde and R. B. Patil, "Optimization of conveyor system components," Int. J. Eng. Res. Appl., vol. 2, pp. 123–129, 2012.

[5] T. Opasiak, D. Gąska, G. Perun, and B. Łazarz, "New design of rollers for belt conveyors," Arch. Transport, vol. 32, pp. 57–67, 2014.

[6] Y. Lu and Q. Li, "A regression model for prediction of idler rotational resistance on belt conveyor," Meas. Control, vol. 52, no. 5–6, pp. 1–11, 2019.

[7] X. Kou, G. Xu, and C. Yi, "Belt-conveyor based efficient parallel storage system design and travel time model analysis," Int. J. Prod. Res., vol. 56, no. 23, pp. 7142–7159, 2018.

[8] P. Kulinowski, P. Kasza, and J. Zarzycki, "Influence of design parameters of idler bearing units on the energy consumption of a belt conveyor," Sustainability, vol. 13, no. 1, art. 437, 2021.

[9] P. Kulinowski, P. Kasza, and J. Zarzycki, "Methods of testing of roller rotational resistance in aspect of energy consumption of a belt conveyor," Energies, vol. 16, no. 1, art. 26, 2023.

[10] L. Gładysiewicz, M. Hardygóra, and W. Kawalec, "Investigation of the dynamic deflection of conveyor belts via experimental and modelling methods," Measurement, vol. 127, pp. 210–220, 2018.

[11] P. M. Kieckhafer, V. Schmid, and P. Spichartz, "A design approach for multiple drive belt conveyors minimizing life cycle costs," J. Clean. Prod., vol. 201, pp. 526–541, 2018.

[12] Y. Feng, M. Zhang, G. Li, and G. Meng, "Dynamic characteristic analysis and startup optimization design of an intermediate drive belt conveyor with non-uniform load," Proc. Inst. Mech. Eng. E, vol. 234, pp. 1–14, 2020.

[13] Z. Wang, K. Hu, Y. Guo, and S. Wang, "Optimization on detent force characteristics of the permanent magnet suspension belt conveyor," Adv. Mech. Eng., vol. 10, pp. 1–12, 2018.

[14] Y. Guo and F. Wang, "Multi body dynamic equations of belt conveyor and the reasonable starting mode," Symmetry, vol. 12, no. 9, art. 1489, 2020.

[15] R. Król, W. Kisielewski, and D. Kaszuba, "Measurements of loads on belt conveyor idlers operated in real conditions," Measurement, vol. 134, pp. 336–344, 2019.

[16] F. Zeng, C. Yan, Q. Wu, and T. Wang, "Dynamic behaviour of a conveyor belt considering non-uniform bulk material distribution for speed control," Appl. Sci., vol. 10, no. 13, art. 4436, 2020.

[17] C. Mitsantisuk et al., "Modeling of twin belt drive conveyor systems," IEEE Trans. Ind. Electron., vol. 56, pp. 1234–1242, 2009.

[18] A. Sabanovic et al., "Modal analysis of belt conveyor dynamic systems," Control Eng. Pract., vol. 12, pp. 145–153, 2004.

[19] A. Hace et al., "Dynamic modeling and resonance control of conveyor systems," Mech. Syst. Signal Process., vol. 21, pp. 2450–2462, 2007.

[20] B. Jeftenic et al., "Dynamic modeling of belt conveyors using Kelvin–Voigt elements," FME Trans., vol. 31, pp. 45–52, 2003.

[21] K. Vijayakumar et al., "Dynamic analysis of long distance conveyor systems," Int. J. Mech. Eng., vol. 4, pp. 89–97, 2012.

[22] A. Wahyudie and H. Kawabe, "Modeling and control of a short DC belt conveyor system," Int. J. Autom. Comput., vol. 8, pp. 321–329, 2011.

[23] R. Król and W. Kisielewski, "Energy efficiency assessment of mining belt conveyors," Min. Sci., vol. 24, pp. 89–101, 2017.

[24] P. Kulinowski and P. Kasza, "Energy consumption analysis of belt conveyor systems," Min. Eng., vol. 61, pp. 112–120, 2020.

[25] Q. Li, Y. Zhang, and H. Wang, "Smart monitoring and predictive maintenance of belt conveyor systems," Sensors, vol. 21, pp. 1–18, 2021.